Raman scattering study of $La_{0.7}Sr_{0.3}MnO_3/SrTiO_3$ multilayers

2002 J. Phys.: Condens. Matter 14 5201

(http://iopscience.iop.org/0953-8984/14/20/315)

INSTITUTE OF PHYSICS PUBLISHING JOURNAL OF PHYSICS: CONDENSED MATTER

J. Phys.: Condens. Matter **14** (2002) 5201–5210 PII: S0953-8984(02)34658-7

Raman scattering study of $La_{0.7}Sr_{0.3}MnO_3/SrTiO_3$ multilayers

J Kreisel[1,4], G Lucazeau[2], C Dubourdieu[1], M Rosina[1,3] and F Weiss[1]

[1] Laboratoire des Matériaux et du Génie Physique, ENS de Physique de Grenoble, BP 46, 38402 St Martin d'Hères Cedex, France
[2] Laboratoire d'Electrochimie et de Physicochimie des Matériaux et des Interfaces, ENSEEG, BP 75, 38402 St Martin d'Hères Cedex, France
[3] Institute of Electrical Engineering, Slovak Academy of Science, 84239 Bratislava, Slovakia

E-mail: jens.kreisel@inpg.fr

Received 8 March 2002
Published 9 May 2002
Online at stacks.iop.org/JPhysCM/14/5201

Abstract

We report room-temperature Raman scattering results on perovskite-type $[(La_{0.7}Sr_{0.3}MnO_3)_m/(SrTiO_3)_n]_{15}$ multilayers, m and n being the thicknesses of layers alternated 15 times. Distinct changes in the Raman spectra for different n and m have been analysed in the light of structural modifications and point to a tensile-strain-induced rhombohedral-to-orthorhombic phase transition in the $La_{0.7}Sr_{0.3}MnO_3$ (LSMO) layers. As a matter of fact, the presented results provide a new structural basis for the earlier proposed magnetic phase separation model. The present work validates tensile strain as an important variable in thin films, which not only allows us to distort the perovskite structure within a crystallographic space group but can readily induce a transition towards another space group and its related physical properties. As shown in this study, the fabrication of superlattice materials then constitutes a powerful method to stabilize such artificial crystal structures (here artificial orthorhombic LSMO at 300 K) over a greater overall thickness than would be possible in single films.

1. Introduction

Hetero-epitaxial structures of oxides have been introduced as promising materials for designing new systems with specific properties, with various perovskite-type $(ABO_3)_n/(A'B'O_3)_m$ multilayers being one of the largest classes of systems currently investigated. One of the key elements that makes multilayer systems attractive is the possible artificial control of structural parameters through strain effects, which can be introduced by lattice mismatch between individual layers and the thickness of the interlayers. Such strain effects have a particularly large impact on multilayers containing perovskites, because perovskites are

[4] Author to whom any correspondence should be addressed.

particularly sensitive to even slight structural modifications [1, 2]. An issue of considerable importance for the understanding of multilayer systems is, just as in bulk samples, resolving how a given perovskite structure evolves with strain and how the observed physical properties relate to the underlying structure.

Unfortunately, modifications of the perovskite structure are often hardly apparent and thus difficult to observe by means of diffraction experiments. As a result of this, but also of the small diffraction volume inherent to thin films, the structure of perovskite layers is often vaguely described as pseudo-cubic or simply admitted to be the same as in the bulk material. Consequently, reliable methods to characterize perovskite-type multilayers are of great interest. Raman spectroscopy is known to be an appropriate technique for the study of subtle structural modifications and has been used for the study of phase transitions in a large number of perovskites. Although Raman spectroscopy has also been shown to be a versatile technique for the characterization of semiconductor multilayers [3], little work has been addressed to $(ABO_3)_n/(A'B'O_3)_m$ superlattices and we are only aware of one Raman spectroscopy study concerning $(PbTiO_3)_n/(BaTiO_3)_m$ multilayers, discussing the possibility of confined modes [4]. Among the various perovskite-type multilayers, those containing $La_{1-x}A_xMnO_3$-type manganites have attracted increasing interest from a fundamental point of view as well as for their relevance in technological applications (see e.g. [5–10] and references therein).

As a starting point of the expected repercussion of the tensile-strain-induced structures on the physical properties in manganite multilayers, it is instructive to consider results from a recent magnetoresistance study of $LSMO_m/STO_n$ multilayers grown by pulsed laser deposition, where a strong coupling between structural (strain-induced) distortion and physical properties has been reported [10, 11]. For decreasing LSMO thickness the main tendencies can be summarized as the following.

(a) The magnetic ordering temperature decreases.
(b) The magnetoresistance of $LSMO_m/STO_n$ multilayers increases considerably with decreasing LSMO thickness.
(c) Samples with very thin LSMO layers become insulating.

According to [10, 11] the latter observations can be understood assuming a magnetic phase separation for the thinnest manganite layers into ferromagnetic–metallic and less ordered insulating clusters. In such a scenario, the electric transport takes place along metallic percolative parts and the insulating behaviour results from the loss of percolation between the metallic regions [10, 11]. The latter proposition is based on recent studies where a magnetic phase separation model (MPSM) has been proposed for doped manganites (see e.g. [12, 13]). In addition to this, a phase-separation-like microstructure has been pointed out in a recent high-pressure study of $LaMnO_3$ (LMO) [14].

While the latter MPSM model was in the beginning regarded as only one (and a controversial one) of the possible interpretations of experimental observations, Bibes *et al* [15] presented very recently direct experimental evidence to support such a view. In their study Bibes *et al* [15] reported on an NMR study evidencing nanoscale multiphase separation at $La_{2/3}Ca_{1/3}MnO_3/SrTiO_3$ interfaces (i.e. at distances < 40 nm from the interface), with each nanoregion having a specific magnetic and electric character. As a matter of fact, their study provides both quantitative and qualitative evidence for such a phase coexistence. While the latter studies investigate only magnetic and electric properties, we shall show in the following a way to explore accompanying structural mechanisms, allowing us to extend our current knowledge on the effect of strain on the structure in perovskite-type multilayers, and the importance of this. In this paper we present a layer-thickness-dependent investigation of

Table 1. Summary of $[(La_{0.7}Sr_{0.3}MnO_3)_m/(SrTiO_3)_n]_{15}$ multilayers investigated in this study, m and n being the thicknesses of layers alternated 15 times.

Formula	Notation in this paper
$[(La_{0.7}Sr_{0.3}MnO_3)_{36}/(SrTiO_3)_{90}]_{15}$	$LSMO_{36}/STO_{90}$
$[(La_{0.7}Sr_{0.3}MnO_3)_{100}/(SrTiO_3)_{90}]_{15}$	$LSMO_{100}/STO_{90}$
$[(La_{0.7}Sr_{0.3}MnO_3)_{210}/(SrTiO_3)_{90}]_{15}$	$LSMO_{210}/STO_{90}$
$[(La_{0.7}Sr_{0.3}MnO_3)_{100}/(SrTiO_3)_{124}]_{15}$	$LSMO_{100}/STO_{124}$

$La_{0.7}Sr_{0.3}MnO_3/SrTiO_3$ multilayers using Raman spectroscopy as a probe of the change in structure. Some preliminary results were presented at the *International Conference on Thin Film Deposition of Oxide Multilayers* in Autrans (France).

2. Synthesis, characterization and experiment

$[(La_{0.7}Sr_{0.3}MnO_3)_m/(SrTiO_3)_n]_{15}$ multilayers, m and n being the thicknesses (in Å) of bi-layers alternated 15 times, were grown at a deposition temperature of 700 °C on $LaAlO_3$ substrates by pulsed-liquid injection metallorganic chemical vapour deposition. After deposition, the superlattices were annealed for 15 min *in situ* at 800 °C under 1 atm of oxygen. A detailed description of the source system and experimental procedure is given elsewhere [16–18]. Three samples with varying LSMO thickness (36, 100 and 210 Å) and constant STO thickness (90 Å) were prepared. Furthermore, in order to study the influence of $SrTiO_3$ thickness, we have synthesized a further superlattice with 100 Å thick LSMO layers and 124 Å thick STO layers; the notation used hereafter for the different superlattices is given in table 1.

Figure 1 presents the x-ray diffraction patterns for different multilayers, which indicate through the observation of satellite peaks a superlattice structure. From these diffraction patterns, it is, however, not possible to determine the exact crystallographic structure of the manganite layers in the superlattices. Finally, because of the LSMO–STO lattice mismatch the LSMO layers are under tensile strain as evidenced by the evolution of lattice parameters [18]. A detailed description of x-ray and magnetic properties is published elsewhere [18].

Raman spectra have been recorded using a Dilor XY multichannel Raman spectrometer, equipped with a liquid-nitrogen-cooled CCD detector. The 514.5 nm line of an Ar^+ ion laser was used as the excitation line. Experiments were conducted in micro-Raman; the light was focused to a 1 μm^2 spot. All measurements performed under the microscope were recorded in a back-scattering geometry; the instrumental resolution was 2.8 ± 0.2 cm^{-1}. Iliev *et al* [19] have reported that Raman spectra of LMO show a strong dependence on the exciting laser power. As a consequence, standard experiments have been carried out using incident powers less than 0.5 mW to avoid structural transformations and overheating. Tests on the multilayers investigated here using an analyser show that only weak polarization effects are present and, thus, for the sake of statistics on the very low scattering intensity, the presented Raman spectra have been obtained in a configuration without polarization analysis. The de-polarization of the Raman diffusion is most probably due to the peculiar microstructure mentioned in the introduction, just as usually observed for another class of micro-structured perovskites: relaxor ferroelectrics.

3. General considerations

In its paraelectric phase above 110 K, $SrTiO_3$ is cubic (O_h space group) and, thus, shows no first-order Raman scattering; its weak and broad Raman spectrum is due to processes involving two phonons, the so-called second-order Raman scattering [20].

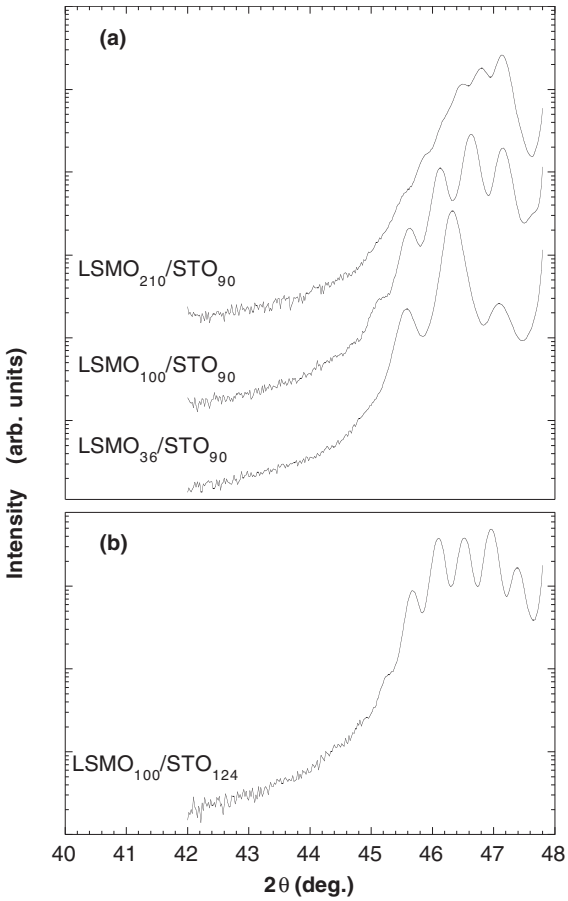

Figure 1. X-ray diffraction pattern (θ–2θ-scans) of $[(La_{0.7}Sr_{0.3}MnO_3)_m/(SrTiO_3)_n]_{15}$ multilayers, m and n being the thicknesses of layers alternated 15 times. The patterns have been shifted for clarity. (a) Multilayers with a $SrTiO_3$ thickness of 90 Å while the LSMO thickness varies from 36 to 210 Å. (b) Multilayer with a $SrTiO_3$ thickness of 124 Å and an LSMO thickness of 100 Å.

Concerning the Sr-doped manganite, it is worth considering first the Raman scattering for the parent compound LMO. At ambient conditions LMO crystallizes in an orthorhombic structure with space group *Pnma* (D_{2h}^{16}). With respect to the ideal cubic perovskite structure the orthorhombic structure is obtained by consequent rotations of the adjacent MnO_6 octahedra about the $[010]_p$ and $[101]_p$ pseudo-cubic axes, leading to the $a^-b^+a^-$ tilt system (Glazer's notation [1, 2]). The 20 atoms in the unit cell of orthorhombic LMO give rise to 24 Raman-active modes [19]:

$$\Gamma_{\text{Raman-orth.}} = 7A_g + 5B_{1g} + 7B_{2g} + 5B_{3g}.$$

At 10 K only 14 of these 24 modes are observed [21]. Although at ambient conditions the spectrum is even less resolved [19], the orthorhombic phase can be identified by its characteristic spectral signature with two intense and dominating Raman peaks at roughly 500 and 600 cm^{-1}.

$La_{1-x}Sr_xMnO_3$, for its part, is known to undergo an orthorhombic-to-rhombohedral (D_{2h}^{16}-to-D_{3d}^{6}) phase transition for $x = 0.17$ [22]. The constituent $La_{0.7}Sr_{0.3}MnO_3$ (LSMO) of the multilayers investigated here is thus expected to show a rhombohedral $R\bar{3}c$ symmetry. Just

as for the orthorhombic case, the rhombohedral structure can be described with respect to the ideal cubic structure, by considering a rotation of MnO_6 octahedra about the $[111]_p$ pseudo-cubic diagonal, leading to the $a^-a^-a^-$ tilt system. The rhombohedral distortion gives rise to five Raman-active modes [23]:

$$\Gamma_{\text{Raman-rhomb.}} = A_{1g} + 4E_g.$$

The Raman scattering intensity of LSMO is considerably reduced with respect to LMO, which has been attributed to a weakening of the Jahn–Teller distortion upon doping, leading to a decreasing deviation from the ideal cubic structure with no first-order Raman scattering [23]. The Raman signature of the orthorhombic-to-rhombohedral transition can be described by a progressive weakening of the two broad and strong 'orthorhombic peaks' (500 and 600 cm^{-1}) [19, 23, 24] and the appearance of two narrow 'rhombohedral peaks' of E_g symmetry (45 and 426 cm^{-1}) [21, 24]. The structure change with increasing Sr content is further accompanied by a low-frequency shift of the band centred at 290 cm^{-1} for LMO to about 180 cm^{-1} for LSMO (see [23]).

4. Results

Figures 2 and 3 present the overall evolution of Raman spectra from $LSMO_m/STO_n$ multilayers for different m and n. Figure 2 focuses on the change in the Raman spectra when the $SrTiO_3$ thickness of the multilayer is maintained constant at 90 Å while the LSMO thickness varies from 36 to 210 Å. The observed Raman bands are rather broad and of weak intensity.

The Raman spectra of the multilayers, except the thickest $LSMO_{210}/STO_{90}$, present a sharp phonon band at 121 cm^{-1} (plus bands at 150 and at 485 cm^{-1} for the thinnest film), which is attributed to the $LaAlO_3$ substrate, thus the Raman spectrum is representative of the whole multilayer. Now, knowing that the observed samples are built up by LSMO and STO layers, a remaining question is to which material the observed bands can be attributed. The comparison with the second-order Raman signature of bulk $SrTiO_3$, given in the literature [20], shows that the remaining bands cannot be attributed to $SrTiO_3$. This is somewhat surprising because the intensity of second-order Raman scattering in $SrTiO_3$ is usually rather strong, but we should recall that the Raman intensity of $SrTiO_3$ in the 200–800 cm^{-1} range is considerably reduced with pressure [25]. As a matter of fact, remembering the above-mentioned spectral characteristics for manganites, the features not belonging to $LaAlO_3$ should be seen as the Raman signature of LSMO layers. In the following, the different spectral changes in $LSMO_m/STO_n$ multilayers will be discussed in the light of this consideration; several qualitative features in the $LSMO_m/STO_n$ Raman spectra can be discerned for changing m and n.

(i) Two broad bands at roughly 500 and 620 cm^{-1}, denoted hereafter D and E, are characteristic for the high-frequency range. Let us recall that this spectral signature is similar to that generally observed for undoped or slightly doped manganites, which adopt an orthorhombic structure. While these bands are the dominating feature of the $LSMO_{36}/STO_{90}$ multilayer, their intensity decreases with increasing thickness of the LSMO; the latter observation is particularly marked for band E.

(ii) B and C around 420 cm^{-1}, which appears only as a very weak shoulder in the Raman spectrum of $LSMO_{36}/STO_{90}$, appears as a clearly distinguishable peak in the Raman spectra of the multilayers containing thicker LSMO layers.

(iii) When the thickness m of the LSMO layer is increased, band A shows a slight low-frequency shift.

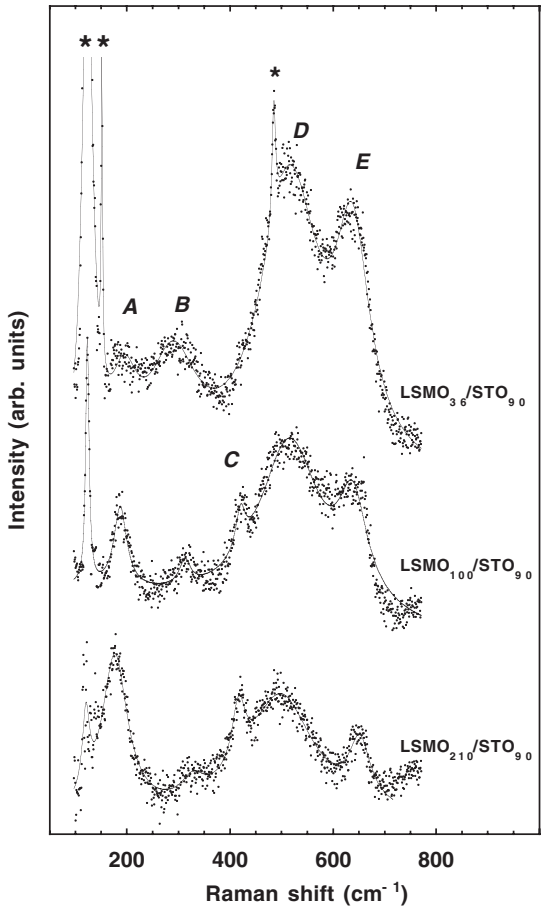

Figure 2. Raman spectra of $[(La_{0.7}Sr_{0.3}MnO_3)_m/(SrTiO_3)_n]_{15}$ multilayers, m and n being the thicknesses of layers alternated 15 times. The results shown here are for multilayers with a $SrTiO_3$ thickness of 90 Å while the LSMO thickness varies from 36 to 210 Å. The spectra have been shifted for clarity. Bands marked with * belong to the $LaAlO_3$ substrate.

As a general matter, each of the points (i)–(iii) mentioned above, describing discontinuous or distinct changes in the Raman spectral features and keeping in mind that Raman spectroscopy is a 'fingerprint' technique, can be seen as an indication of a thickness-dependent structural modification in $LSMO_m/STO_n$ multilayers.

5. Spectral analysis

5.1. $LSMO_m/STO_{90}$

Let us first discuss the spectral evolution of $LSMO_m/STO_{90}$, i.e. multilayers where the $SrTiO_3$ thickness is maintained constant at 90 Å and the LSMO thickness m is changing.

As stated above, one of the marked features of the Raman spectra on $LSMO_{36}/STO_{90}$ is the observation of two phonons in the 450–650 cm^{-1} range, which points to an orthorhombic lattice distortion of the 36 Å thin LSMO layer. Since bulk LSMO is known to adopt a rhombohedral structure [22] this is somewhat surprising, and we attribute this observation to non-negligible tensile-strain-induced effects.

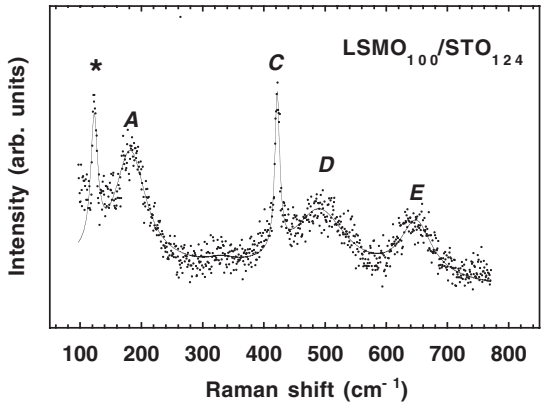

Figure 3. Raman spectra of a $[(La_{0.7}Sr_{0.3}MnO_3)_{100}/(SrTiO_3)_{124}]_{15}$ multilayer. Bands marked with * belong to the $LaAlO_3$ substrate.

Now, when the thickness of the LSMO layer is increased to $LSMO_{100}/STO_{90}$ or $LSMO_{210}/STO_{90}$ the Raman spectra are significantly different. First, the intensity of the 'orthorhombic' bands D and E is clearly reduced (although still persistent); such a spectral change is known to accompany an orthorhombic-to-rhombohedral transition [19, 23, 24]. Further to the intensity change, one can note a slight low-frequency shift of bands D and E with increasing LSMO thickness. Based on temperature-dependent Raman spectra, Podobedov *et al* [23] were the first to assign such an anomaly to a spin–phonon interaction, the softening being then the result of a magnetic rearrangement. It is tempting to interpret our observation in a similar way but this will need further investigations beyond the scope of this work. Second, band A displays two changes with increasing LSMO thickness: (a) a clear intensity enhancement, which can again be attributed to a transition towards a rhombohedral structure [24], and (b) an important negative frequency shift from 195 cm^{-1} ($LSMO_{36}/STO_{90}$) to 176 cm^{-1} ($LSMO_{210}/STO_{90}$). The latter frequency shift is understood by considering that band A corresponds to rotations of the MnO_6 octahedra [19] and, thus, such a negative frequency shift should be attributed to a change in the octahedron tilt system.

Nevertheless, the evolution of bands A, D and E does not provide a sufficient criterion for a structural transition, since it does not allow us to distinguish a reduced orthorhombic lattice distortion from a clear transition towards a rhombohedral structure. In fact, the strongest argument for an evolution towards a new rhombohedral structure arises from the third marked spectral change, the appearance of a new phonon centred at $\approx$420 cm^{-1}, which is known as the predominant Raman spectral signature of a rhombohedral structure in manganites [21,24]. The observation of a rhombohedral distortion for $LSMO_{100}/STO_{90}$ or $LSMO_{210}/STO_{90}$ is well understood and even expected by considering that multilayers with increasing LSMO thickness are closer to bulk material, which presents a rhombohedral structure.

We need to discuss whether the LSMO layers in $LSMO_{100}/STO_{90}$ or $LSMO_{210}/STO_{90}$ are purely rhombohedral. Iliev *et al* [19] have reported Raman spectra of 'rhombohedral' LMO showing among other bands still also broad bands at 490 and 610 cm^{-1}, which would indicate the possibility of true rhombohedral LSMO layers. However, in a more recent study it has been objected that purely rhombohedral manganites do not show broad bands at 490 and 610 cm^{-1} and that the observation of these bands in the rhombohedral phase is due to surface degradation at the manganite–air interface [21]. As a consequence, it is important to emphasize that the final layer of the $LSMO_m/STO_n$ multilayers studied here is $SrTiO_3$, acting so to speak as a protective layer, and thus the observed 'orthorhombic' bands at 490 and 610 cm^{-1} should be seen as an

intrinsic signature of the LSMO layers. Therefore, the simultaneous observation of phonons at 420, 490 and 620 cm^{-1} seems to indicate the coexistence of competing rhombohedral and orthorhombic crystallographic structures. With respect to the latter, it is worth pointing out that the intensity of the individual bands changes when going from $LSMO_{100}/STO_{90}$ to $LSMO_{210}/STO_{90}$, i.e. the intensity increases for bands A and C, while bands B, D and E decrease. The latter observation is most probably related to a decrease of the orthorhombic fraction to the profit of an increase of the rhombohedral fraction in the LSMO layer.

5.2. $LSMO_{100}/STO_n$

It is now interesting to turn to the case where the thickness of the LSMO layer is maintained but the thickness of the $SrTiO_3$ layer is increased, i.e. to compare Raman spectra of $LSMO_{100}/STO_{90}$ and $LSMO_{100}/STO_{124}$.

As shown in figure 3, increasing the thickness of the STO layer resembles the above-described effect for bands A, B, D and E when the thickness of the LSMO layer is increased. In particular, the intensity of bands D and E is clearly reduced with increasing STO thickness, pointing to a reduced (almost no longer present) proportion of orthorhombic parts in the film and thus indicating strain release through thicker $SrTiO_3$ layers. Another remarkable observation, when comparing $LSMO_{100}/STO_{90}$ and $LSMO_{100}/STO_{124}$, is observed for band C, which shows for the $LSMO_{100}/STO_{124}$ multilayer a decrease in the width at half maximum (FWHM), leading to a striking sharp phonon band. Bearing in mind that a change in the FWHM of a Raman band is inversely proportional to the lifetime of the corresponding phonon, the latter observation points to a well established long-range rhombohedral distortion.

6. Microstructure in strained $LSMO_m/STO_n$ multilayers

6.1. Rhombohedral–orthorhombic coexistence

The spectral analysis in the above sections 5.1 and 5.2 gives evidence for a tensile-strain-induced structural evolution of LSMO layers in $LSMO_m/STO_n$ heterostructures, from 'bulk-rhombohedral' $LSMO_{100}/STO_{124}$ to 'tensile-strain-stabilized' orthorhombic $LSMO_{36}/STO_{90}$, going through multilayers which show a somewhat rhombohedral–orthorhombic coexistence. A remaining question is how to imagine the rhombohedral–orthorhombic coexistence. On the basis of our measurements, we unfortunately cannot distinguish a phase separation between the STO–LSMO interface and the inner part of the LSMO layer from a microstructure presenting orthorhombic and rhombohedral phase separations. However, if we follow the interpretations by Bibes *et al* [15], this might favour a cluster-like (i.e. phase segregation) picture. As pointed out by Kimura *et al* [26], such a picture with clusters in a somewhat different matrix is reminiscent of the suggested microstructural picture for so-called relaxor ferroelectrics (relaxors), which have been studied for years. As a matter of fact, based on a study of Cr-doped $Nd_{1/2}Ca_{1/2}MnO_3$, Kimura *et al* [26] have recently proposed the term 'relaxor ferromagnet' for doped manganites which show typical relaxor-features such as in-field annealing, aging and microstructural phase separation.

6.2. Rhombohedral-to-orthorhombic phase transition

As a general matter, the rhombohedral ($R\bar{3}$)-to-orthorhombic (*Pbnm*) (R $\rightarrow$ O) phase transition is one of the common phenomena in manganites. From a crystallographic point of view the latter transition can be described by a change in the tilt of the MnO_6 octahedra ($a^-a^-a^-$ to $a^-b^+a^-$), leading to a decrease in the Mn–O–Mn bond angle. It has already been shown that for

$La_{1-x}Sr_xMnO_3$ external parameters such as temperature and/or chemical substitution [22, 27] or magnetic field [28] can introduce an R → O transition. On the other hand, the present study has shown that tensile stress leads equally to an R → O phase transition and, thus, from a crystallographic point of view, appears to act similarly to decreasing Sr doping or lowering temperature. As a general matter, such R → O phase transitions are known to have an important impact on the physical properties of manganite-type perovskites.

Above we have suggested a phase separation-type microstructure, but how should we imagine these regions? On the basis of magnetic and electrical transport properties the authors of [10, 11] have ruled out a structural or magnetic phase transition as the origin of the enhanced MR, but propose regions with different magnetic and transport properties. The latter proposition is based on recent studies where an MPSM has been proposed for doped manganites (see e.g. [12, 13]). In contrast, our present investigation by Raman spectroscopy suggests a layer-thickness-dependent structural modification through a regime of phase coexistence, most probably in the form of rhombohedral and orthorhombic regions. We believe that the two latter models for $LSMO_m/STO_n$ multilayers are by no means in disagreement or exclude each other but reflect rather the different characteristics of magnetic measurements (average, magnetic properties), transport measurements (average, electric properties) and Raman spectroscopy (local, structural properties).

If we now assume a picture of a phase-separation-like microstructure as suggested by our and the cited literature studies, it seems intuitive to attribute a magnetic (magnetic or less ordered), electric (metallic or insulating) and structural (rhombohedral or orthorhombic) property for at least two, or according to Bibes *et al* [15] even more, types of region. On a hypothetical basis we might propose two regions, A and B: A might be *rhombohedral–metallic–ferromagnetic*, with properties like those of bulk LSMO and dominating thick LSMO; B might be *orthorhombic–insulating* and show a different magnetic ordering from A. In such a description the magnetic and electric part arises from the studies reported in [10, 11] and by Bibes *et al* [15] while the structural part arises from the present Raman study. We should, however, parenthesize that the films investigated by Bibes *et al* [15] are Ca doped and do not adopt the rhombohedral structure, which makes a direct comparison difficult. Nevertheless, if we admit that the reported structural phase separation is something characteristic in manganites (just as for the famous relaxor ferroelectrics, as pointed earlier), the observed average structure (rhombohedral or not) does not play an important role, but rather the observation of local deviation from the ideal cubic structure which is likely to be present in the samples studied by Bibes *et al* [15].

One of the structural mechanisms which one might take into consideration to explain the sort of balancing described in the above three steps can be based on the intuitive image of chemically different regions A and B. Such chemically different regions would have, on a microscopic level, different compressibilities [29], which then implies that the two regions evolve differently under strain. Finally it is tempting to compare the effect of high pressure on bulk materials with the effect of strain in thin films. However, such a comparison is not straightforward since the strain in thin films is not hydrostatic as in the studies of bulk material. Nevertheless, it is interesting to note that somewhat similar phase separations and phase transition mechanisms have been observed in pressure-dependent studies on manganite-type oxides; the interested reader should refer to [14, 30–32].

7. Concluding remarks

In the present work we have reported on an investigation of $LSMO_m/STO_n$ multilayers by Raman spectroscopy, which points to a tensile-strain-induced rhombohedral-to-orthorhombic

structural modification in LSMO layers. As a matter of fact, our results show that the reported changes [10, 11] in the physical properties of $LSMO_m/STO_n$ are accompanied by a structural phase transition and, thus, a description by the so-called *magnetic phase separation model*, as proposed in [10, 11], needs to be extended by structural arguments/descriptions. Our work validates tensile stress as an important variable, which not only allows us to distort the perovskite structure within a crystallographic space group but can readily induce a transition towards another space group and its related physical properties. Then, the fabrication of superlattice materials constitutes a powerful method to stabilize such artificial crystal structures and physical properties over a greater thickness than would be possible in simple films. We suggest enlarging the study of multilayers systematically by local structural probes such as Raman spectroscopy, which we have shown to be a good candidate for such an analysis in manganites.

Acknowledgments

The authors are grateful to Dr K Dörr (IFW Dresden, Germany) and colleagues for information about their magnetoresistance study on $LSMO_m/STO_n$ and a preprint of the corresponding presentation at *EMSA 2000* in Dresden.

References

[1] Glazer A M 1972 *Acta Crystallogr.* B **28** 3384
[2] Glazer A M 1975 *Acta Crystallogr.* A **31** 756–62
[3] Ruf T 1998 *Phonon Raman Scattering in Semiconductors, Quantum Wells and Superlattices (Springer Tracts in Modern Physics)* (Stuttgart: Springer) p 249
[4] Le Marrec F, Farhi R, El Marssi M, Dellis J L, Karkut M G and Ariosa D 2000 *Phys. Rev.* B **61** R6447–50
[5] Gong G Q, Gupta A, Gang X, Lecoeur P and McGuire T R 1996 *Phys. Rev.* B **54** R3742–5
[6] Jo M H, Mathur N D, Evetts J E, Blamire M G, Bibes M and Fontcuberta J 1999 *Appl. Phys. Lett.* **75** 3689–91
[7] Ueda K, Tabata H and Kawai T 1999 *Phys. Rev.* B **60** R12 561–4
[8] Venimadhav A, Hegde M S, Prasad V and Subramanyam S V 2000 *J. Phys. D: Appl. Phys.* **33** 2921–6
[9] Panagiotopoulos I, Christides C, Pissas M and Niarchos D 2001 *J. Mater. Process. Technol.* **108** 193–6
[10] Walter T *et al* 2001 *Sensors Actuators* A **91** 184–7
[11] Dörr K *et al* 2001 *J. Appl. Phys.* **89** 6973–5
[12] Moon Ho J, Mathur N D, Todd N K and Blamire M G 2000 *Phys. Rev.* B **61** R14 905–8
[13] Fath M, Freisem S, Menovsky A A, Tomioka Y, Aarts J and Mydosh J A 1999 *Science* **285** 1540–2
[14] Loa I *et al* 2001 *Phys. Rev. Lett.* **82** 125501
[15] Bibes M B *et al* 2001 *Phys. Rev. Lett.* **87** 67 210
[16] Sénateur J P, Weiss F, Thomas O, Madar R and Abrutis A 1993 Patent No 93/08838
[17] Sénateur J P, Dubourdieu C, Weiss F, Rosina M, Abrutis A 2000 *Adv. Mater. Opt. Electron.* **10** 155–61
[18] Dubourdieu C, Rosina M, Roussel H, Weiss F, Sénateur J P and Hodeau J L 2001 *Appl. Phys. Lett.* **79** 1246
[19] Iliev M N *et al* 1998 *Phys. Rev.* B **57** 2872–7
[20] Fleury P A, Scott J F and Worlock J M 1968 *Phys. Rev. Lett.* **21** 16
[21] Granado E *et al* 1998 *Phys. Rev.* B **58** 11 435–40
[22] Urushibara A *et al* 1995 *Phys. Rev.* B **51** 14 103–9
[23] Podobedov V B, Weber A, Romero D B, Rice J P and Drew H D 1998 *Phys. Rev.* B **58** 43
[24] Bjornsson P *et al* 2000 *Phys. Rev.* B **61** 1193–7
[25] Grzechnik A, Wolf G H and McMillan P F 1997 *J. Raman Spectrosc.* **28** 885–9
[26] Kimura T, Tomioka Y, Kumai R, Okimoto Y and Tokura T 1999 *Phys. Rev. Lett.* **83** 3940–3
[27] Tokura Y *et al* 1994 *J. Phys. Soc. Japan* **63** 3931–5
[28] Asamitsu A, Moritomo Y, Tomioka Y, Arima T and Tokura Y 1995 *Nature* **373** 407–9
[29] Kreisel J and Glazer A M 2000 *J. Phys.: Condens. Matter* **12** 9689–98
[30] Srinivasan G and Hanna D 2001 *Appl. Phys. Lett.* **79** 641
[31] Khazeni K, Jia Y X, Li L, Crespi V H, Cohen M L and Zettl A 1996 *Phys. Rev. Lett.* **76** 295–8
[32] Garbarino G *et al* 2001 *J. Magn. Magn. Mater.* **226** 843–4